Astron. Astrophys. 195, 301–309 (1988)

ASTRONOMY AND ASTROPHYSICS

Dynamics of sub-relativistic electron beams in magnetic traps: A model for solar N-bursts

A. Hillaris[1], C.E. Alissandrakis[1], and L. Vlahos[2]

[1] Section of Astrophysics, Astronomy and Mechanics, Department of Physics, University of Athens, GR-15783 Athens, Greece
[2] Section of Astrophysics, Astronomy and Mechanics, Department of Physics, University of Thessaloniki, GR-54006 Thessaloniki, Greece

Received July 27, accepted October 20, 1987

Summary. The dynamic evolution of mildly relativistic electrons (10–100 keV) injected into a model magnetic trap is studied numerically, using the drift approximation. Wave-particle interactions are neglected, since the beam plasma system is shown to be non-linearly decoupled in the range of parameters used in our study. The results from this simulation are used to interpret certain observational characteristics of the N-bursts observed by the Nançay radio spectrograph. N-bursts are believed to be the first direct radio evidence for mirror effects in solar magnetic loops.

Key words: Sun: type III bursts – N-bursts – Sun: particle trapping – beam-plasma interaction

1. Introduction

Type-U radio bursts trace the propagation of beams of mildly relativistic electrons along closed magnetic field lines (coronal loops). They appear as an inverted letter U on the dynamic spectrum recordings. The radio emission first drifts rapidly towards lower frequencies and after reaching a turnover point (minimum frequency or maximum altitude of the beam) the ascending branch is followed by a descending branch towards higher frequencies.

Certain observations made with the Digital Multichannel Radiospectrograph of the Space Research Laboratory of the Observatory of Paris (Dumas et al., 1982) revealed a third ascending branch following the type-U event, thus suggesting the capital letter N on the dynamic spectrum. A detailed analysis of the time profiles showed that the duration of the beam emission regularly increased with time along the three successive branches of the so called N-burst, thus suggesting that the event was produced by the same electron beam and demonstrating that N bursts actually trace reflections on magnetic mirrors near the coronal loop foot points (Caroubalos et al., 1987).

The time profile of a type III, U- or N-bursts at a given frequency is believed to represent the passage of the electron beam through that frequency level. The burst duration is believed to be related to the length of the exciter and was found to correlate well with the distance from the source (see Poquérusse et al., 1984 for these types of bursts). The N-bursts were found to have a typical total duration of 10 s in the frequency range 400–150 MHz, while the half power duration of the time profiles increased regularly along each of the three branches and continuously from one branch to the next. The injection time of the beam was estimated to be of the order of 0.7 ± 0.2 s.

The purpose of this article is to present a number of simulations of the propagation of electron beams in magnetic traps, which can interpret certain characteristics of the observed N-bursts. In Sect. 2 we use a simple model to demonstrate that under conditions characteristic of the solar corona, electron beams can be treated as almost free streaming in the ambient plasma, while the level of the Langmuir wave excited has a power law dependence on the beam density. Our analysis is based on a set of equations for the non linear wave-wave interaction introduced by Vlahos and Rowland, (1984). In Sect. 3 we simulate the dynamics of a free streaming electron beam in a simple magnetic trap model. Examining the resulting instantaneous density-time profiles of the beam at various points, we reproduce the temporal and spatial evolution of the type N event. The results of the simulation are used to interpret observational characteristics of the N-bursts such as the increase of their duration as a function of time, the intensity-time profile and the average dynamic spectrum.

2. The non-linear evolution of the beam plasma system

In the linear regime the beam-plasma system is unstable. Plasma waves W_k with phase velocities $v_{ph} = \omega_e/k \leq v_b$ will grow at a rate γ_L, where:

$$\gamma_L = (N_b/N)(v_b/\Delta v_b)^2 \omega_e. \quad (1)$$

In this expression N is the density of the ambient plasma, N_b the density of the beam with an average velocity v_b and a velocity dispersion Δv_b.

The resonant Langmuir waves diffuse the beam particles in velocity space towards lower velocities, forming a quasi-plateau for the beam distribution (Zheleznyakov and Zaitsev, 1970). The quasilinear evolution of a beam interacting with the ambient plasma is described by the following set of equations:

$$\left(\frac{\partial}{\partial t} + v\frac{\partial}{\partial s}\right) f_b = \frac{\partial}{\partial v} D \frac{\partial}{\partial v} f_b - \nu_c f_b \quad (2a)$$

$$\frac{\partial W_k}{\partial t} = \gamma_L W_k, \quad (2b)$$

Send offprint requests to: A. Hillaris

where $D=(4\pi e/m)^2\ W_k/v$ (see for example Ryutov and Sagdeev, 1970), W_k is the spectral energy density of the Langmuir waves and ν_c a Krook collision term (see for example Sanderson, 1981; Bhatnagar et al., 1954).

The main assumption of the Eq. (2) is that the mode coupling terms are negligible, thus the energy density W_k grows linearly. The quasi-linear approximation is based on the assumption that the bump formed on the tail of the ambient plasma distribution has a very low density (Gronard, 1982), otherwise the mode coupling terms cannot be neglected.

The dominant non-linear mode coupling process results from the Langmuir-ion acoustic wave coupling via the ponderomotive force (Zakharov, 1972). This coupling can efficiently transfer the energy of the resonant Langmuir wave into lower phase velocities. In addition, the growing ion acoustic modes can scatter Langmuir waves out of resonance with the beam; when such processes take place in a time interval less than the characteristic time for the generation of the beam-resonant waves, the level of wave energy resonantly interacting with the beam remains low at all times (Papadopoulos, 1975; Papadopoulos et al., 1974; Smith et al., 1979). Thus Eq. (2b) is replaced by a set of equations describing the growth, damping and transfer of energy in various wave modes (Goldstein et al., 1979).

In this article we make use of an approximate model (Vlahos and Rowland, 1984) which describes wave-wave interactions by making use of the total energy density of the modes. This is valid for the ion-acoustic waves as well as for the resonant and non resonant Langmuir waves, which have a well separated spectrum. According to the above model, Eq. (2b) becomes:

$$\partial W_1/\partial t=\gamma_L W_1-\gamma_{NL} W_2 W_1^{1/2}\theta(W_1-W_{th})-a_{NL} W_3 W_1\theta(W_3-W_2) \quad (3a)$$

$$\partial W_2/\partial t=\gamma_{NL} W_2 W_1^{1/2}\theta(W_1-W_{th})-\gamma_L W_2-a_{NL} W_3 W_2\theta(W_3-W_2) \quad (3b)$$

$$\partial W_3/\partial t=\gamma_{NL} W_2 W_1^{1/2}\theta(W_1-W_{th})-\nu_1 W_3\theta(W_3-W_2), \quad (3c)$$

W_1, W_2, W_3 are the total energy densities for the resonant, the non resonant and ion-acoustic wave respectively, $\gamma_{NL} W_1^{1/2}=\omega_e(m/M)^{1/2}(W_1/N\kappa T_e)^{1/2}$ is the non linear energy transfer rate (Papadopoulos, 1975) and $a_{NL} W_3=\omega_e(k_d/k_s)^2(W_3/N\kappa T_e)$ is the scattering rate of Langmuir waves on ion sound oscillations (Dawson and Oberman, 1962)

Equations (3) can be made dimensionless by measuring time in ω_e^{-1} and normalizing energy densities to $N\kappa T_e$. The step function $\theta(W_1-W_{th})$ models the presence of a threshold, $W_{th}/N\kappa T_e$, in the nonlinear instability, while $\theta(W_3-W_2)$ models the effect of the conversion of ion acoustic density fluctuations into normal modes and vice-versa. When the non resonant Langmuir waves, W_2, are damped, ion density fluctuations convert into normal ion acoustic waves and can be damped as well, while for a high level of W_2, an almost stationary non linear ion acoustic perturbation is obtained (Rowland, 1980). The terms ν_1 and ν_L represent the Landau damping rates by the ambient plasma for ion acoustic and Langmuir waves respectively.

Solving Eqs (3) for a broad range of parameters characteristic for type N, U and III events in the solar corona we can show that W_1 either follows a spiky pattern or reaches a quasi steady state, depending on the values of ν_L (which is a function of T_e/T_i) and γ_L. A spiky behaviour is expected when the beam density is high and $\gamma_L>\nu_1$; in this case W_1 will reach a value much higher than the threshold before W_3 reaches an appreciable level. Subsequently the Langmuir waves are very efficiently scattered by ion density fluctuations and quickly drop below the threshold. The ion acoustic waves decay slowly and reach a point where the growth of the primary waves is possible again, thus resetting the system. When ν_1 is comparable to γ_L the scattering of the Langmuir waves follows the variations of W_1; thus when the driving term $\gamma_L W_1$ falls, W_3 also falls and vice versa, hence leading to the establishment of a quasi steady state.

Typical examples of the time evolution of the wave levels are shown in Fig. 1. The value of W_1 averaged over a time interval of the order of 0.1 s, (the time resolution of the Nançay Radiospectrograph) justifies the assumption that the diffusion term D in Eq. (2a) is negligible (we will return to this point later in the text).

Thus Eq. (2a) can be rewritten in the form:

$$\left(\frac{\partial}{\partial t}+v\frac{\partial}{\partial s}\right)f_b=-\nu_c f_b. \quad (3d)$$

In Eq. (3d) the phenomenological term ν_c for the effective collision frequency includes both Coulomb collisions and collisions on ion acoustic density fluctuations. Hence ν_c is written as the sum of two terms, $\nu_c=\nu_{cc}+\nu_{ci}$, where:

$$\nu_{cc}=4\pi N_e^4 L(\mu_i e^{-2}+\mu_{ee})/v^3 \quad (4a)$$

(see for example Ishimaru, 1986); μ_{ie} and μ_{ee} are the reduced masses for the electron-electron and electron-ion collisions respectively, and

$$\nu_{ci}=k_s\lambda_d W_3/N\kappa T_e(v_e/v)^3\omega_e, \quad (4b)$$

(Papadopoulos, 1977).

We begin our analysis by solving Eq. (3d) using for the computation of ν_{ci} an initial estimate for W_3; from the value and the initial parameters of the streaming beam we obtain v_b, Δv_b, N_b/N at every point in space and time. These values are used for computing γ_L and W_{th} (see above) which are in turn used in the solution of the rate Eqs. (3a–3c). The obtained value of W_3, averaged over space and time is checked against the initial estimate and if the difference is greater than half an order of magnitude the process is repeated until the convergence of system (3).

The model used in this simulation is one dimensional with homogeneous magnetic field. In the calculation we assumed that 10^{13} particles with a temperature of $2.7\ 10^8$ K were initially contained in a region of 10^5 km long. Since the assumed temperature corresponds to a thermal velocity of $0.3c$, this treatment is equivalent to assuming that we have an injection time of the order of 1 s.

The electron-ion temperature ratio was assumed equal to 5, since direct measurements in the solar wind (Lin et al., 1986) showed that $T_e/T_i\sim 5$. The threshold for the oscillating two stream instability (OTSI) was assumed to be of the order of $10^{-6}\ N\kappa T_e$ (see also Fig. 1c). In the calculation the scale length for the ambient plasma density was taken equal to 10^5 km, a reasonable assumption for coronal conditions.

The self-consistency of the solution requires a check of the assumptions initially made, i.e. that the inverse of the characteristic time for quasi-linear relaxation is much less than the collision frequency and that the total energy lost to the waves is much smaller than the total beam energy. The time for quasi linear

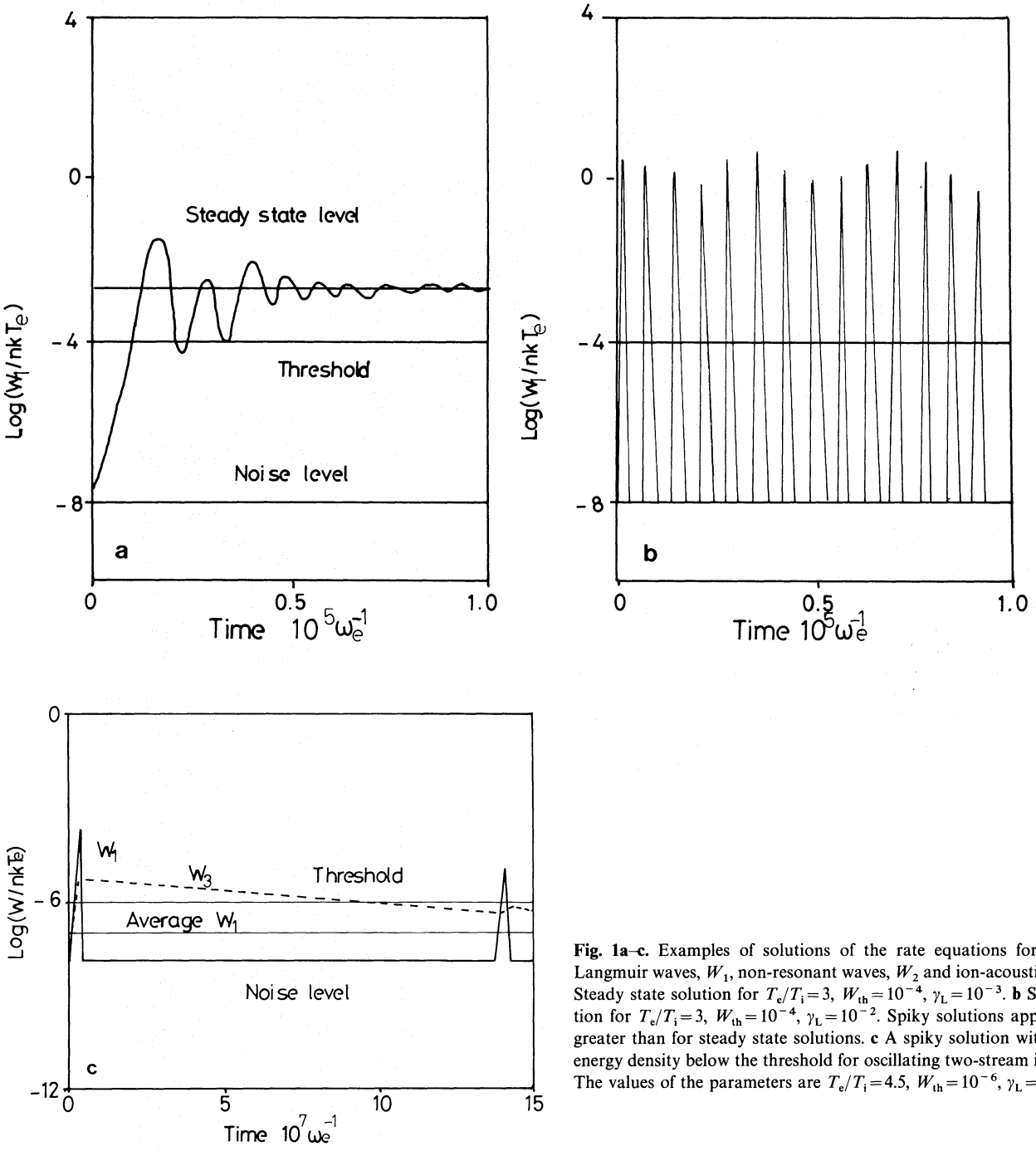

Fig. 1a–c. Examples of solutions of the rate equations for resonant Langmuir waves, W_1, non-resonant waves, W_2 and ion-acoustic waves. **a** Steady state solution for $T_e/T_i=3$, $W_{th}=10^{-4}$, $\gamma_L=10^{-3}$. **b** Spiky solution for $T_e/T_i=3$, $W_{th}=10^{-4}$, $\gamma_L=10^{-2}$. Spiky solutions appear for γ_L greater than for steady state solutions. **c** A spiky solution with average energy density below the threshold for oscillating two-stream instability. The values of the parameters are $T_e/T_i=4.5$, $W_{th}=10^{-6}$, $\gamma_L=5\,10^{-5}$

relaxation, T_{ql}, was estimated as

$$T_{ql}^{-1} \simeq \frac{\partial}{\partial v} D \frac{\partial}{\partial v} \simeq \frac{D}{v^2} \simeq (4\pi e/m)^2 W_1/v^3, \quad (5)$$

which gives $T_{ql}^{-1} \simeq 2.1\ 10^{28}/v^3\ s^{-1}$ for the parameters adopted, while the calculated value of W_1 is of the order of $10^{-7}\ N\kappa T_e$ at the most.

The collision frequency of beam electrons with ion sound was calculated assuming $k_s\lambda_d \simeq 2\pi/10$ (see for example Vlahos and Rowland, 1984), $\omega_e=5.7\ 10^8\ s^{-1}$ (for the assumed value of $N=10^8\ cm^{-3}$) and $W_3/N\kappa T_e \simeq 10^{-6}$ as found in the simulation. The resulting value for the collision frequency is $\nu_{ci} \simeq 7.5\ 10^{28}/v^3\ s^{-1}$, while the Coulomb collision term was calculated assuming $L \simeq 23$ (Spitzer, 1962) as $\nu_{cc} \simeq 0.7\ 10^{28}/v^3$. Hence the total collision term was $\nu_c \simeq 8.2\ 10^{28}/v^3$, which is greater than T_{ql}^{-1}.

The total energy of the beam lost to the wave excitation during the streaming between $s=2.5\ 10^5$ km and $s=4.5\ 10^5$ km, where s is the distance from the injection point, was computed from:

$$E_{waves} = \int\int W_1 \gamma_L ds dt$$

and was up to 23% of the total beam energy. The point at $2.5\ 10^5$ km was selected because, due to the large injection time, it

takes almost $2.5\,10^5$ km for the thermal cloud to form a well defined beam, while $4.5\,10^5$ km is a reasonable estimate for the length of the loop.

The values calculated above for plasma wave energy and T_{ql}^{-1} give rough upper limits of the beam losses, because we have computed W_1 assuming W_3 (ion sound) to be at the noise level ($10^{-10}\,N\kappa T_e$); a more detailed calculation would give greater values for W_3, since the inverse of the damping rate ν_1 is comparable to the time required for a significant change in the beam parameters ($\nu_1^{-1} \simeq 0.1$ s).

From the solution of the rate Eqs. (3) it is clear that the levels of W_1, W_2 and W_3 depend on the beam parameters, as well as on those of the ambient plasma due to the dependence of the coefficients γ_L, a_{NL}, ν_L and ν_1 on v_b, Δv_b, N_b/N and ω_e. In particular W_1, which is considered as the main source of the fundamental radiation, was found to vary as γ_L^a (the exponent, a, depending mainly on T_e/T_i) for a wide range of parameters. For a wide range of γ_L values (10^{-4} to $10^{-6.5}$) W_1 and γ_L were found to have a dependence of the form:

$$\log(W_1/N\kappa T_e) = -2.98 + 0.83 \log(\gamma_L/\omega_e),$$

while W_2 is almost independent of γ_L with a value of $\sim 10^{-8}\,N\kappa T_e$. The level of ion sound waves also shows a power law dependence on γ_L, of the form:

$$\log(W_3/N\kappa T_e) = -1.11 + 1.04 \log(\gamma_L/\omega_e).$$

The results are shown in Fig. 2.

The average level of the resonant Langmuir wave is almost half an order of magnitude below the threshold for the oscillating two stream instability (OTSI), but non linear effects have still a very important part in the beam stabilization process, since the peaks of W_1 are well above W_{th}, due to the spiky structure of the solution of Eq. (3) (cf. Fig. 1c).

From the calculations we found that there is a power law dependence of the level of the resonant Langmuir wave and the beam-ambient plasma density ratio (Fig. 3). A linear regression analysis gave the approximate relation:

$$W_1/N\kappa T_e \propto (N_b/N)^{2.05}. \quad (9)$$

The same type of dependence is deduced from the approximate analytical solution of the rate equations both in the case of steady state and in the spiky case (see Appendix).

A similar power-law dependence has been observed in the solar wind type III bursts (Fitzenreiter et al., 1976) and was confirmed by solving the nonlinear beam plasma equations for a fully evolved exciter (Smith et al., 1976) for typical solar wind parameters.

Hence we conclude that, in a first order approximation, we are justified to treat the exciter of the type N and U bursts as a free streaming beam for distances of the order of $2\,10^5$ km and to simulate these types of events by computing time profiles of the beam density at every point.

3. The free streaming of mildly relativistic electrons in magnetic traps

In Sect. 2 we showed that, for a wide range of parameters characteristic of the type III, U and N events, the drift approximation is satisfactory. In addition, the level of plasma waves

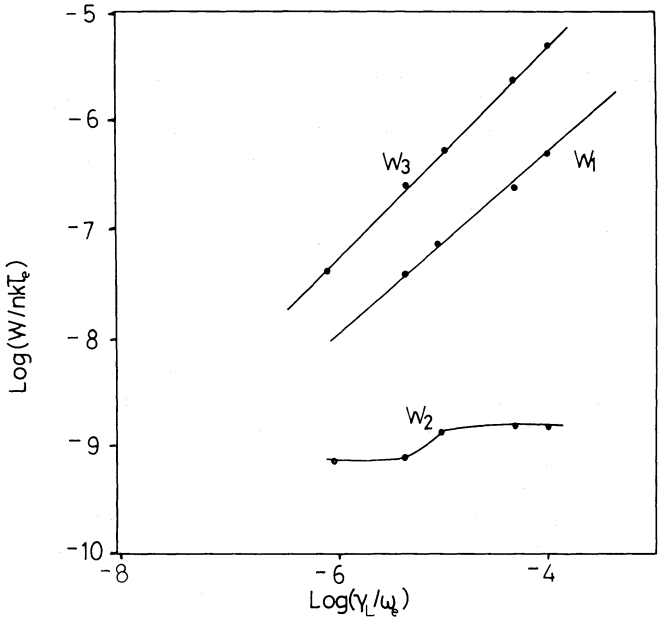

Fig. 2. Average levels of Langmuir and ion acoustic wave as a function of γ_L/ω_e, with $T_e/T_i = 5$ and $W_{th} = 10^{-6}$. In this parameter regime only spiky solutions of the rate equations were obtained

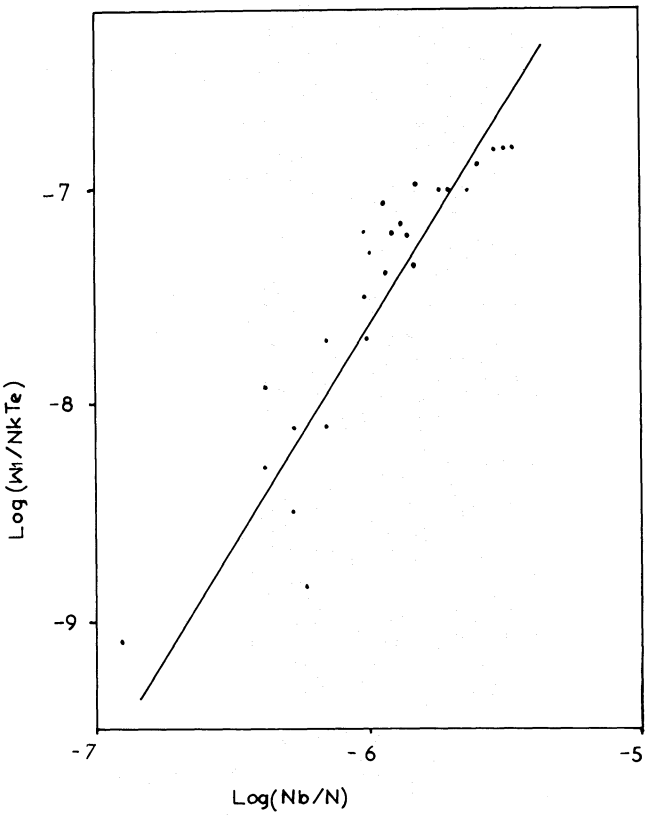

Fig. 3. Langmuir wave energy versus the ratio of beam to ambient plasma density for the beam parameters used. The scatter of the data points is due to the variation of the linear growth rate γ_L which is related to the ratio $v_b/\Delta v_b$. If a diffusion in velocity space term had been included, it would have smoothed out $v_b/\Delta v_b$ variations giving a better power law fit

excited by the beam was shown to have a power law dependence on the beam density, i.e. $W_1 \propto N_b^a$. In this section we present results of simulations of electron beams streaming in magnetic trap configurations in an attempt to interpret certain observational characteristics of the N-bursts.

The following equation describes the beam dynamics in the trap:

$$\frac{d}{dt} f_b(s, v, t) = -v_c f_b(s, v, t), \tag{10}$$

where (Kovalev and Korolev, 1981):

$$\frac{d}{dt} \equiv \frac{\partial}{\partial t} + v\cos\theta \frac{\partial}{\partial s} - v \frac{\partial B}{ds} \frac{\sin^2\theta}{2B} \frac{\partial}{\partial \cos\theta},$$

θ is the pitch angle, s the coordinate along the trap and v_c a phenomenological term including both Coulomb collisions and collisions on ion density fluctuations in the sense described in Sect. 2. The first and second term of the convective derivative describe temporal and spatial variations, while the third describes the longitudinal component of the Lorentz force. In the calculations the value of v_c was estimated as almost 2π times the Coulomb collision frequency (see discussion in the previous section).

The characteristics of the homogeneous equation, $df_b/dt = 0$ are: The total energy, the adiabatic invariant, μ, and the quantity

$$C = t + \int \frac{ds}{\sqrt{(v^2 - 2\mu B/m_e)}}. \tag{11}$$

Assuming a parabolic law of variation for the magnetic field, $B = B_0(1 + as^2)$ (see for example Vilmer et al., 1985), we obtain from (11):

$$C = t \pm \sin^{-1}\{s\sqrt{ma/(v^2 - m)}\}/\sqrt{ma}, \tag{12}$$

where $m = 2\mu B_0/m_e$.

The above analysis implies that electrons oscillate along the trap with bounce frequency proportional to $\sqrt{\mu}$ and the expected general solution is of the form:

$$\Psi = \Psi'(\mu, v, C)\exp(-v_c t), \tag{13}$$

where Ψ' can be any function, but in the subsequent analysis it will be determined from the initial conditions of the problem. We note that Ψ' (but not Ψ) preserves the total number of electrons in the beam, while the instantaneous beam density is

$$N_b(s, t) = 2\pi \iint \Psi dv_\parallel v_\perp dv_\perp. \tag{14}$$

In the magnetic traps studied, which model coronal loops, we expect a fraction of the initial population to escape out of the trap and collisionally thermalize into the dense chromospheric plasma, while the rest of the initial population will remain trapped, forming a loss cone distribution.

The analytical solution presented above does not account for the cut-off of the electrons which overcome the loop length L, while in the numerical calculations these electrons are removed. The fraction of the electrons remaining in the trap after the first reflection is

$$p = 2\pi \int_{-\infty}^{\infty} ds \int_{-\infty}^{\infty} dv_\parallel \int_{|v_\parallel|\gamma}^{\infty} \Psi_0 v_\perp dv_\perp \tag{15}$$

where Ψ_0 is the initial distribution, while the parameter γ defines the loss cone in $v_\parallel$, $v_\perp$ space and is given by $\gamma = \sqrt{(B_{max}/B_{inj} - 1)^{-1}}$.

For an initial distribution in the form of a maxwellian in $v_\parallel$ $v_\perp$, with an average parallel velocity $v_\parallel'$ the fraction of trapped electrons is given, for a narrow injection, by:

$$p = \exp\left(-x^2 \frac{1-\lambda^2}{\lambda^2}\right) \Big/ \lambda \tag{16}$$

where $x = v_\parallel/\Delta v$ and $\lambda = \sqrt{(1 + \gamma^2 T/T)}$. The above treatment implies that the initial energy spectrum of the injected electrons must be of the form of a power law or a hot maxwellian because, otherwise, the losses due to precipitation at the foot-points of the trap will be severe and the reflected branch will not appear.

The numerical solution of the free streaming equations was performed by solving the equations of motion for a single particle, thus determining its initial velocity and position in terms of its current position and velocity. The resulting expressions are entered into the initial distribution function, giving the distribution function at every point, at any time, in terms of $v_\parallel$ and $v_\perp$. The initial beam distribution is taken as a thermal cloud, expanding through an ambient plasma of density 10^8 cm^{-3} and temperature of 10^6 K.

Examples of the velocity distributions obtained in this way are given in Fig. 4. In the computed $v_\parallel$ $v_\perp$ contours the ratio $|v_\parallel/v_\perp|$ has always a lower limit, $[B_{inj} - B)/B]^{-1/2}$, due to the preservation of the adiabatic invariant μ, while for the reflected electrons there is also an upper limit due to the loss cone, equal to $(B_{max}/B - 1)^{-1/2}$. The resulting distribution $\Psi'(s, v_\parallel, v_\perp, t)$ is integrated over $v_\parallel$ and $v_\perp$ to give the beam density at every point, at a specified time. In Fig. 4a we show the streaming part of the beam at the point $s = -1.8\ 10^5$ km (the origin is at the top of the loop). This velocity distribution agrees with the result of Winglee and Dulk (1986). It is important to note that collisions will slow down the low velocity electrons. In Fig. 4b we show the velocity distribution just before the reflection region $s = 1.8\ 10^5$ km, at $t = 6$ s and in Fig. 4c the velocity distribution just after the reflection.

For computational convenience the calculations were made using a very short impulsive injection, with an injection region 1% of the loop length. The results were subsequently reduced to injections of finite duration of the order of 0.5 s by performing a convolution of the beam density over the duration of the injection. The initial parameters, i.e. the injection time and the thermal velocity of the cloud were chosen to comply with the total duration of the observed events. The collisional term, v_c, was taken almost 6 times the Coulomb collision frequency in order to account for the collisions of particles with ion acoustic density fluctuations.

The resulting density-time profiles (Fig. 5a) resemble strongly the intensity-time profiles of type U- and N-bursts (Poquerusse et al., 1984; Caroubalos et al., 1987). Each panel in Fig. 5a corresponds to a fixed frequency of observation and shows separate plots for the ascending (branch 1), descending (branch 2) and reflected (branch 3) electrons. The decay part is almost exponential with a slope that decreases with time. Near the top of the loop (middle of the trap) there is a significant overlap of the ascending and descending branches, while a similar effect can be seen in the descending and reflected branches near the feet of the loop (cf. Fig. 4 of Caroubalos et al., 1987).

On the basis of the computed time profiles we calculated the half power duration, D, as a function of the peak time, T (Fig. 5b).

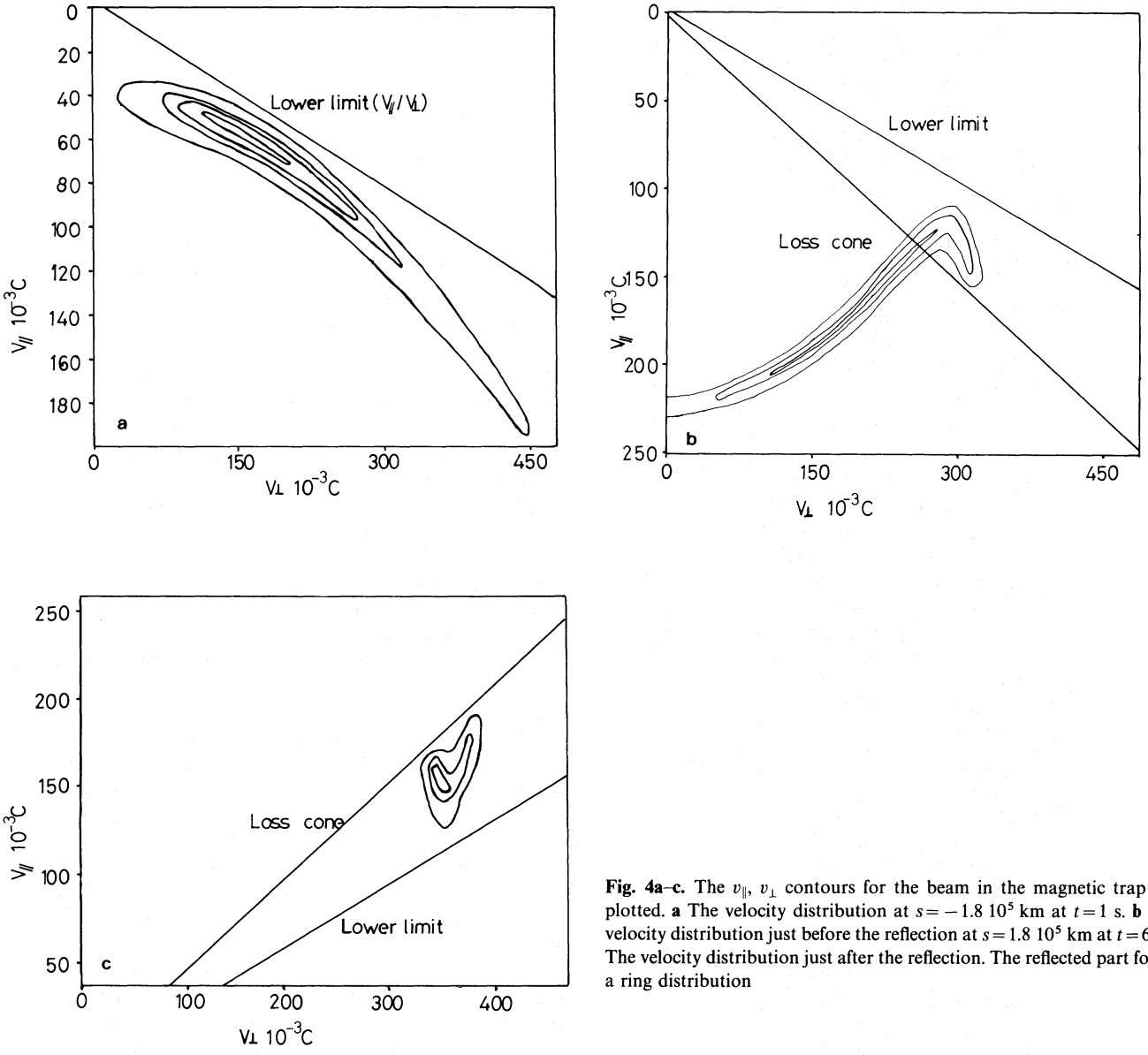

Fig. 4a–c. The $v_{\|}$, $v_{\perp}$ contours for the beam in the magnetic trap are plotted. **a** The velocity distribution at $s=-1.8\ 10^5$ km at $t=1$ s. **b** The velocity distribution just before the reflection at $s=1.8\ 10^5$ km at $t=6$ s. **c** The velocity distribution just after the reflection. The reflected part forms a ring distribution

Table 1. Parameters of model loops

No.	Loop length (10^5 km)	Temperature (10^7 K)	Injection point (10^5 km)	B_{max}/B_{min}	Trapped particles (%)	Duration-time parameters A (s)	B
1	2	1.7	−0.975	10	21	0.88	0.15
2	3	3.8	−1.46	10	21	1.11	0.18
3	4	6.7	−1.95	10	21	0.96	0.29

These parameters were observed to have an almost linear dependence of the form $D_{obs}=D_s+0.22\ T_{obs}$, where $D_s=0.7\pm0.2$ s (Caroubalos et al., 1987, their Fig. 7). Table 1 gives the values of the parameters used in the simulation and the coefficients A and B from the linear regression analysis of the relation between the computed half power duration and time. As shown in the table, the calculated values are in very good agreement with the observed ones for various parameters of the model loop.

The results of the simulation for model 3 of Table 1 are shown in the form of a "dynamic spectrum" in Fig. 6, where we have

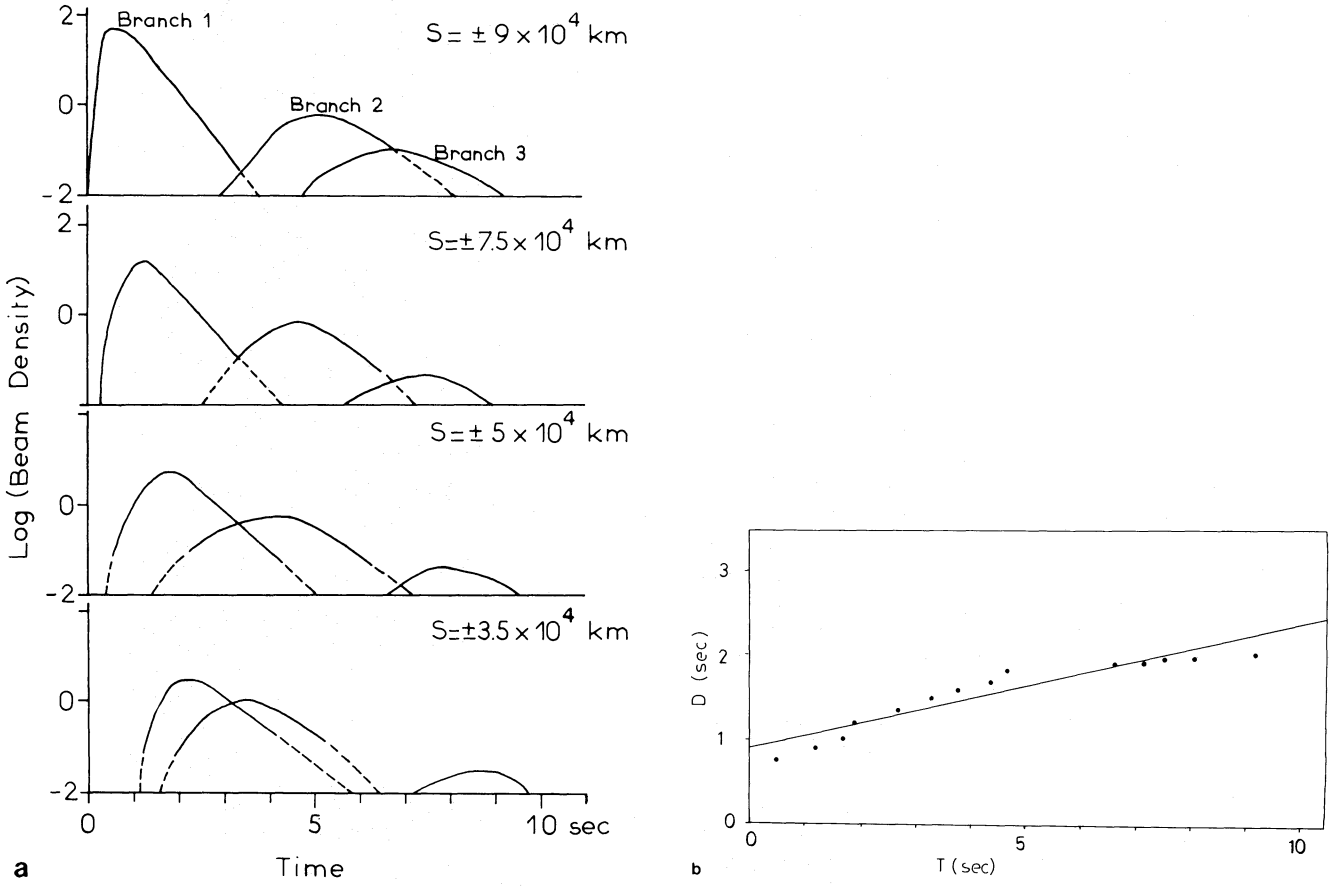

Fig. 5. **a** Time profiles of the beam density for a thermal cloud ($1.7\ 10^7$ K temperature) expanding in a symmetric loop $2\ 10^5$ km long at various positions in the loop. The beam is injected in a region located $9.7\ 10^4$ km away from the center of the trap. Distance is measured from the centre of the trap which corresponds to the top of the loop. Branches 1, 2 and 3 correspond to ascending, descending and reflected electrons. Upgoing, downgoing and reflected electrons at symmetric positions with respect to the top of the loop have been plotted in the same panel; these points are located at the same height in the corona and hence they are expected to emit radio waves at the same frequency. Thus the plots mimic the dynamic spectrum of N bursts. **b** Plot of the half power duration of the beam at a particular position, D, as a function of peak time, T, for the thermal cloud of Fig. 5a

plotted the time of maximum beam density at different heights in the loop (continuous line) for the three branches; the loop was assumed semicircular in shape. The linear height scale in Fig. 6 corresponds to a logarithmic frequency scale in the observed dynamic spectra. Also in Fig. 6 we have plotted the times at which the beam density rises to one half of its maximum value and the time at which it drops to that level again (shaded region). The figure shows a remarkable similarity with Fig. 10 of Caroubalos et al. (1987) which was obtained from the analysis of N-burst observations.

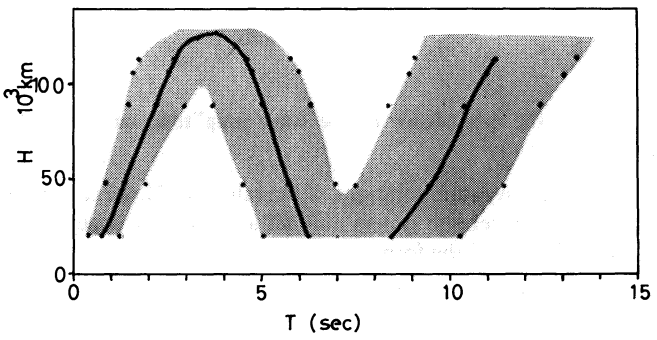

Fig. 6. Peak time (continuous line) and half power duration (shaded region) as a function of height above the footprints of the loop for model 3 of Table 1; the loop has been assumed semicircular for simplicity. The picture clearly suggests the dynamic spectrum of an N-burst

4. Summary and conclusions

In this paper we presented results of numerical calculations for electron clouds streaming in magnetic traps, in an attempt to simulate the N-bursts observed with the Digital Multichannel Radiospectrograph of the Space Research Laboratory of the Observatory of Paris (Caroubalos et al., 1987).

Using the approach of the rate equations developed by Vlahos and Rowland (1984) we showed that under coronal conditions a thermal cloud injected at one end of a large loop with length of the order of $2\ 10^5$ km with an injection time of the order of 1 s can be treated using the free streaming drift approximation because it looses only a small fraction of its energy into waves. The inverse time for diffusion into velocity space is estimated to be small, compared to the collision frequency.

The level of plasma wave excited was shown to have a power law dependence on the beam density, while we expect the intensity of the fundamental electromagnetic radiation to have also a power law dependence on the Langmuir wave energy density (Smith and Davis, 1975). Therefore we presume that density-time profiles give an approximate picture of the intensity-time profiles observed at various frequencies with the radiospectrograph.

We proceeded with the computation of density-time profiles of a thermal cloud expanding in a model magnetic trap, taking into account the precipitation of electrons at the footprints of the trap. Our model accounts reasonably well for the observed time profiles, the total duration of the event and its dynamic spectrum. The qualitative agreement between the observed and calculated characteristics provides strong evidence in favor of the hypothesis that the same electron beam successively produces the three branches of N-bursts. Hence we conclude that N-bursts are a manifestation of a magnetic mirror effect on beams of mildly relativistic electrons under solar corona conditions.

A more refined model is required to account for the effects of diffusion in velocity space which may become important as the beam propagates, forming anisotropies in $v_\parallel$, $v_\perp$ space. The Langmuir, whistler and lower hybrid waves excited in this way tend to smooth out the anisotropies formed. We expect that the reflected ring distribution will be unstable to whistler and lower hybrid waves. It is important to incorporate the local evolution of the reflected particles due to waves in out model. This work is in progress.

The collisional term used in a rough phenomenological approximation, while a Fokker-Planck type term (Kovalev and Korolev, 1981) would give more accurate results, including electron losses due to pitch angle scattering into the loss cone; however this Fokker-Planck type term should account for collisions of the streaming electrons with ion acoustic density fluctuations as well as for Coulomb collisions.

Acknowledgements. We thank Prof. C. Caroubalos and Dr J.-L. Bougeret for many helpful discussions. This work was supported in part by the Greek General Secretariat for Research and Technology.

Appendix: the dependence of the wave amplitude on the beam density

Assuming steady state solutions of the rate eqs. (3), we can solve the resulting algebraic system and get a power law dependence for W_1 and W_2 of the form:

$$W_1/N\kappa T_e=(\gamma_L/\gamma_{NL})^2\propto(N_b/N)^2$$

$$W_1/N\kappa T_e=(\gamma_L/\gamma_{NL})\propto N_b/N$$

where the constants depend on $V_b/\Delta V_b$.

In the case of spiky solutions we can average over a time interval such that the time derivatives of W_1, W_2 and W_3 vanish due to the quasi periodic behaviour of the solutions. The rate equations give for this case:

$$\gamma_L\langle W_1\rangle=\gamma_{NL}\langle W_2\sqrt{W_1}\theta(W_1-W_{th})\rangle-a_{NL}\langle W_1 W_3\rangle \quad (A1)$$

$$0=\gamma_{NL}\langle W_2\sqrt{W_1}\theta(W_1-W_{th})\rangle-a_{NL}\langle W_2 W_3\rangle \quad (A2)$$

$$0=\gamma_{NL}\langle W_2\sqrt{W_1}\theta(W_1-W_{th})\rangle-\nu_1\langle W_3\rangle \quad (A3)$$

where we have omitted the small term $\nu_1 W_2$ and $\langle\ \rangle$ denote time averages. Since W_3 is weakly damped we have assumed that $\theta(W_3-W_2)=1$ during the averaging period. In addition, since W_2 and W_3 attain high values only when $W_1>W_{th}$ we can take the corresponding theta function equal to unity. Further simplifications can be made because, although W_1, W_2 and W_3 reach their peak values almost simultaneously, W_2 varies much faster than W_1 which varies much faster than W_3 (cf. Fig. 3 of Vlahos and Rowland, 1984). Therefore it is reasonable to assume that

$$\langle W_1 W_3\rangle\simeq\langle W_1\rangle W_{3max}=\langle W_1\rangle\langle W_3\rangle X_3$$

$$\langle W_2 W_3\rangle\simeq\langle W_2\rangle\langle W_3\rangle X_3$$

$$\langle W_2\sqrt{W_1}\rangle\simeq\langle W_2\rangle\sqrt{W_{1max}}=\langle W_2\rangle\sqrt{\langle W_1\rangle X_1}$$

where X_1 and X_3 are constants because W_1, W_2 and W_3 are periodic. Under these assumptions Eqs. (A1) to (A3) become:

$$\gamma_L\langle W_1\rangle=\gamma_{NL}X_1\langle W_2\rangle\sqrt{\langle W_1\rangle}-a_{NL}X_3\langle W_1\rangle\langle W_3\rangle \quad (A4)$$

$$0=\gamma_{NL}X_1\langle W_2\rangle\sqrt{\langle W_1\rangle}-a_{NL}X_3\langle W_2\rangle\langle W_3\rangle \quad (A5)$$

$$0=\gamma_{NL}X_1\langle W_2\rangle\sqrt{\langle W_1\rangle}-\nu_1\langle W_3\rangle \quad (A6)$$

Solving these equations we obtain:

$$\langle W_1\rangle\simeq(\gamma_L/\gamma_{NL}X_1)^2 \quad (A7)$$

$$\langle W_2\rangle=(\nu_1/a_{NL}X_3) \quad (A8)$$

$$\langle W_3\rangle\simeq(\gamma_L/a_{NL}X_3) \quad (A9)$$

From which we see that the average value of W_1 is proportional to the square of the beam density (through γ_L), the average value of W_2 does not depend on the beam density, while W_3 is proportional to the beam density. The parameters X_1 and X_3 depend on the ratio of the pulse duration to the pulse period.

The above dependence of W_3 on γ_L expresses the balance between the growth rate of W_1 and its scattering on the ion acoustic fluctuations, without taking into account the small mode coupling term. The dependence of W_3 expresses the balance between the energy transfer rate to the non resonant mode W_2 and the scattering of that mode on the ion sound wave.

References

Bhatnagar, P.L., Gross, E.P., Krook, M.: 1954, *Phys. Rev.* **94**, 511
Caroubalos, C., Poquéruse, M., Bougeret, J.L., Crepel, R.: 1987, *Astrophys. J.* **319**, 503
Dawson, J.M., Oberman, C.: 1962, *Phys. Fluids* **5**, 517
Dumas, G., Caroubalos, C., Bougeret, J.L.: 1982, *Solar. Phys.* **81**, 383
Fittzenreiter, R., Evans, L., Lin, R.: 1976, *Solar Phys.* **46**, 437
Goldstein, M., Smith, R., and Papadopoulos, K.: 1979, *Astrophys. J.* **234**, 683
Gronard, R.J.: 1983, *Solar, Phys.* **83**, 207
Ishimaru, S.: 1986, *Plasma Physics. an Introduction to Statistical Physics of Charged Particles*, Benjamin/Cunning Publ. Co., California
Kovalev, V., Korolev, O.: 1981, *Sov. Astron.* **25**, 215
Lin, R.P., Levendahl, W.K., Lotko, W., Gurnett, O.A., Scarf, F.L.: 1986, *Astrophys. J.* **308**, 954
Papadopoulos, K., Goldstein, M., Smith, R.: 1974, *Astrophys. J.* **190**, 175

Papadopoulos, K.: 1975, *Phys. Fluids* **18**, 1769
Papadopoulos, K.: 1977, *Rev. Geophys. Space Phys.* **15**, 173
Poquérusse, M.: 1977, *Astron. Astrophys.* **56**, 251
Poquérusse, M., Bougeret, J.L., Caroubalos, C.: 1984, *Astron. Astrophys.* **136**, 10
Rowland, H.: 1980, *Phys. Fluids* **5**, 517
Ryutov, D.D., Sagdeev, R.Z.: 1980, *Soviet Phys. JETP* **31**, 396
Sanderson, J.J.: 1981, in R.D. Gill, ed., *Plasma Physics and Nuclear Fusion Research*, Academic Press, London
Spitzer, L.: 1962, *Physics of Fully Ionized Gases*, Wiley Interscience, New York
Smith, D., Davis, W.: 1975, *Solar Phys.* **41**, 439
Smith, R., Goldstein, M., Papadopoulos, K.: 1979, *Astrophys. J.* **190**, 175
Vlahos, L., Rowland, H.: 1984, *Astron. Astrophys.* **139**, 263
Vilmer, N., Trottet, G., Mac Kinnon, A.: 1986, *Astron. Astrophys.* **156**, 64
Winglee, R., Dulk, C.: 1986, *Astrophys. J.* **307**, 808
Zacharov, V.E.: 1972, *Soviet Phys. JETP* **35**, 908
Zheleznyakov, V.V., Zaitsev, V.V.: 1970, *Soviet Astron.* **14**, 250